



Deposited via The University of Leeds.

White Rose Research Online URL for this paper:

<https://eprints.whiterose.ac.uk/id/eprint/97642/>

Version: Published Version

Article:

Barkov, MV and Komissarov, SS (2011) Recycling of neutron stars in common envelopes and hypernova explosions. *Monthly Notices of the Royal Astronomical Society*, 415 (1). pp. 944-958. ISSN: 1365-2966

<https://doi.org/10.1111/j.1365-2966.2011.18762.x>

This article has been accepted for publication in *Monthly Notices of the Royal Astronomical Society* ©: 2011 Author(s) Published by Oxford University Press on behalf of the Royal Astronomical Society. All rights reserved

Reuse

Items deposited in White Rose Research Online are protected by copyright, with all rights reserved unless indicated otherwise. They may be downloaded and/or printed for private study, or other acts as permitted by national copyright laws. The publisher or other rights holders may allow further reproduction and re-use of the full text version. This is indicated by the licence information on the White Rose Research Online record for the item.

Takedown

If you consider content in White Rose Research Online to be in breach of UK law, please notify us by emailing eprints@whiterose.ac.uk including the URL of the record and the reason for the withdrawal request.

Recycling of neutron stars in common envelopes and hypernova explosions

Maxim V. Barkov^{1,2,3*} and Serguei S. Komissarov^{2*}

¹Max-Planck-Institut für Kernphysik, Saupfercheckweg 1, 69117 Heidelberg, Germany

²Department of Applied Mathematics, The University of Leeds, Leeds LS2 9JT

³Space Research Institute, 84/32 Profsoyuznaya Street, Moscow 117997, Russia

Accepted 2011 March 21. Received 2011 March 14; in original form 2010 December 22

ABSTRACT

In this paper, we propose a new plausible mechanism of supernova explosions specific to close binary systems. The starting point is the common envelope phase in the evolution of a binary consisting of a red supergiant and a neutron star. As the neutron star spirals towards the centre of its companion it spins up via disc accretion. Depending on the specific angular momentum of the gas captured by the neutron star via the Bondi–Hoyle mechanism, it may reach millisecond periods either when it is still inside the common envelope or after it has merged with the companion core. The high accretion rate may result in the strong differential rotation of the neutron star and generation of the magnetar-strength magnetic field. The magnetar wind can blow away the common envelope if its magnetic field is as strong as 10^{15} G and can destroy the entire companion if it is as strong as 10^{16} G. The total explosion energy can be comparable to the rotational energy of a millisecond pulsar and reach 10^{52} erg. However, only a small amount of ^{56}Ni is expected to be produced this way. The result is an unusual Type II supernova with very high luminosity during the plateau phase, followed by a sharp drop in brightness and a steep light-curve tail. The remnant is either a solitary magnetar or a close binary involving a Wolf–Rayet star and a magnetar. When this Wolf–Rayet star explodes, it will be a third supernova explosion in the same binary.

Key words: stars: magnetars – stars: neutron – supernovae: general.

1 INTRODUCTION

Usually, neutron stars (NSs) have magnetic field $B \sim 10^{12}$ G and rotate with a period of a fraction of a second, the Crab pulsar being a typical example. However, we now know that the ‘zoo’ of NSs is much more diverse and they can have both much weaker and much stronger magnetic field and rotate with both much longer and much shorter periods.

Around 10 per cent of NSs have the surface dipolar magnetic field $B \sim 10^{14}$ – 10^{15} G (Kouveliotou et al. 1998). These ‘magnetars’ are believed to be born in core-collapse explosions of rapidly rotating stars. During the collapse, the proto-NS naturally develops strong differential rotation, which allows for the generation of magnetic field via α – Ω dynamo (Duncan & Thompson 1992; Thompson & Duncan 1993). The strength of the saturated magnetic field strongly depends on the rotational period, with shorter periods leading to stronger magnetic field and more rapid release of rotational energy. In order to generate the magnetar-strength magnetic field, the rotation period must be around few milliseconds (Duncan & Thompson 1992). Such a strong field allows to release up to 10^{52} erg of the

magnetar’s rotational energy in very short period of time. This is sufficient to drive extremely powerful supernova explosions, on the hypernova scale, and to produce powerful gamma-ray bursts (GRBs, e.g. Usov 1992; Thompson, Chang & Quataert 2004). The turbulence required for the magnetic dynamo action can also be generated via the magnetorotational instability (Balbus & Hawley 1991). Calculations based on the linear theory show that in the supernova context strong saturation field can be reached very quickly on the time-scale of only several tens of rotational periods (Akiyama et al. 2003; Obergaulinger et al. 2009).

Millisecond pulsars are found in low-mass binaries, and it is generally thought that they have been spun up via disc accretion (Alpar et al. 1982; Archibald et al. 2009). This origin implies mass increase by about $0.2 M_{\odot}$ compared to normal radio pulsars, whose masses are narrowly distributed around $1.35 M_{\odot}$ (Thorsett & Chakrabarty 1999). It is rather difficult to measure the mass of a millisecond pulsar, but the few available results agree with this prediction of the accretion model (Kaspi, Taylor & Ryba 1994; Jacoby et al. 2005; Demorest et al. 2010). The most massive pulsar found to date, almost $2 M_{\odot}$, is a millisecond pulsar (Demorest et al. 2010). The magnetic field of these millisecond pulsars is very low, down to 10^9 G. Most likely, their initial magnetic field was of similar strength to normal pulsars, but now it is buried under the layers of accreted matter (Bisnovatyi-Kogan & Komberg 1974; Alpar et al. 1982).

*E-mail: bmv@maths.leeds.ac.uk (MVB); serguei@maths.leeds.ac.uk (SSK)

The reason why these pulsars could not generate magnetar-strength magnetic field in the same way as in the core-collapse scenario is the very long time-scale of spinning up compared with the viscous time-scale. As a result, the differential rotation remains weak and there is not enough energy for effective magnetic dynamo (Spruit 1999).

The rotational frequency of the fastest X-ray pulsar is ~ 760 Hz (Chakrabarty et al. 2003), whereas the fastest known radio pulsar has the frequency of 641 Hz (Backer et al. 1982). Most likely, it is the gravitational radiation loss what places the upper limit on the rotation rates because at high spin the r -mode oscillations become excited (Shapiro & Teukolsky 1983; Levin 1999). Spruit (1999) argued that this instability may also result in magnetic explosions. The idea is that the heating of NSs, associated with these oscillations, reduces their viscosity and decouples its interior from the outer layers. Being most disturbed, the outer layers rapidly lose some of their angular momentum via gravitational radiation. This leads to strong differential rotation and the generation of the magnetar-strength magnetic field in the NS interior. This field becomes unstable to buoyancy, emerges on the surface, and the magnetically driven pulsar wind rapidly extracts the rotational energy of the NS. Spruit (1999) proposed this as an alternative scenario for long GRBs. It is unlikely that a supernova-like event can accompany a GRB in this scenario. Although the wind energetics are sufficient, only a small fraction of this energy can be deposited into the companion star, simply because of its small geometrical cross-section. Moreover, recent results suggest that the amplitude of r modes may saturate at a much lower level due to non-linear interaction with other modes (Arras et al. 2003; Brink, Teukolsky & Wasserman 2005; Bondarescu, Teukolsky & Wasserman 2007).

A similar recycling of NSs may occur during the common-envelope (CE) phase, after the primary becomes a red supergiant (RSG; Bisnovatyi-Kogan & Syunyaev 1971; Paczynski 1976; Tutukov & Yungelson 1979; Postnov & Yungelson 2006). Due to the dynamic friction, the NS then spirals inside the RSG, accreting on its way. Now one can imagine two interesting outcomes of such processes. First, the NS may accumulate too much mass and collapse into a black hole (BH). This BH is likely to be rapidly rotating and drive a stellar explosion in the collapsar fashion (Fryer & Woosley 1998; Zhang & Fryer 2001; Barkov & Komissarov 2010).

Secondly, the NS may first spin up to a millisecond period and drive a magnetic explosion of the type proposed by Spruit (1999) but now inside the CE. The magnetar wind can keep energizing such supernovae, producing a similar effect to radioactive decay (Kasen & Bildsten 2010; Woosley 2010). High accretion rates may modify the way the NS is recycled. The accreted gas can form a massive rapidly rotating layer above the NS crust (Inogamov & Sunyaev 1999, 2010). The strong differential rotation between the layer and the NS core may result in the development of the Kelvin–Helmholtz instability when the NS crust melts down under the weight of the layer. This may lead to the turbulence and strong amplification of the NS magnetic field.

The accretion on to NSs during the in-spiral has been studied by Chevalier (1996) who concluded that the high angular momentum of the gas gravitationally captured by a NS prevents it from effective neutrino cooling and keeps the mass-accreting rate well below the rate of the Bondi–Hoyle capture. As a result, the NS accumulates very little mass while still inside the CE. On the other hand, he suggested that during the merger with the companion core the mass accretion rate rises and the NS collapses into a BH. While carefully analysing various effects of rotation, Chevalier (1996) did not use any particular model for the primary. Moreover, there is a great

deal of uncertainty as regards the specific angular momentum of the gravitationally captured gas. In our study, we come back to this problem, consider realistic models of RSG stars and allow for the uncertainty.

This paper is organized as follows. In Section 2, we consider the accretion and recycling of NSs during the in-spiral. We conclude that the outcome is very sensitive to the assumed specific angular momentum of the gravitationally captured gas. Given the current uncertainty as regards the angular momentum, it seems possible that NSs begin to accrete with the Bondi–Hoyle rate while still inside CEs. In this case, they rapidly spin up to millisecond periods. In Section 3, we speculate on the possible mechanisms of generating magnetar-strength magnetic field and study the magnetic interaction of millisecond magnetars with accretion flows typical for the in-spiral problem. We find that if the magnetar forms inside the CE and its magnetic field is about 10^{15} G, the magnetospheric pressure can overcome the gravity and drive an outflow, with eventual release of up to 10^{52} erg of the magnetar rotational energy. If the magnetar forms only after the merger with the core, then higher magnetic field, $\sim 10^{16}$ G, is required to drive stellar explosions. In Section 4, we discuss the properties of such explosions and their observational signatures. Because the RSG envelope is rich in hydrogen, the supernova will be classified as Type II. Because of the very high energy release and relatively small mass of the RSG, the speed of the ejecta is expected to be very high, $\sim 10^9$ cm s $^{-1}$, and the luminosity at the plateau phase $\sim 10^{43}$ erg s $^{-1}$. However, due to the small amount of ^{56}Ni generated in the explosion and the rapid spin-down of the magnetar, the plateau is followed by a sharp drop in brightness and a steep light-curve tail. We show that the termination shock of the magnetar wind produces a high-energy synchrotron and inverse-Compton (IC) emission which may energize the tail, but the supernova ejecta soon becomes transparent to this emission, limiting its potential to mimic the effect of radioactive decay. The flux of gamma-ray emission is expected to be rather low and difficult to observe, unless the explosion occurs in the Local Group of galaxies. In the case of the off-centre explosion, the remnant is a very close binary system consisting of a Wolf–Rayet (WR) star and a magnetar, but the strong magnetic field prevents the magnetar from accreting the plasma of the WR wind. Our results are summarized in Section 5.

In this paper, the dimensional estimates are presented using the following notations: the time $t_{x,n}$ is measured in 10^n s, the distance $R_{x,n}$ in 10^n cm, the speed $V_{x,n}$ in 10^n cm s $^{-1}$, the mass $M_{x,n}$ in $10^n M_{\odot}$, the mass accretion rate $\dot{M}_{x,n}$ in $10^n M_{\odot}$ yr $^{-1}$ and the magnetic field $B_{x,n}$ in 10^n G.

2 IN-SPIRAL DYNAMICS AND RECYCLING OF NEUTRON STARS

As the neutron spirals inside its giant companion, it accretes mass and angular momentum. The accretion can proceed at the Eddington rate or at the much higher Bondi–Hoyle rate. This depends on whether the radiation is trapped in the accretion flow and the neutrino cooling is sufficiently effective (Houck & Chevalier 1991; Chevalier 1993, 1996; Fryer, Benz & Herant 1996). Only if the accretion proceeds at the Bondi–Hoyle rate that the recycling of NSs is sufficiently fast and the explosion can occur during the in-spiral.

In the Bondi–Hoyle problem, an accreting point mass M is moving with a finite speed v_{∞} through a uniform medium of mass density ρ_{∞} and sound speed $c_{s,\infty}$. The Bondi–Hoyle mass accretion

rate is well approximated by the equation

$$\dot{M}_{\text{BH}} = \pi R_{\text{A}}^2 \rho_{\infty} v_{\infty}, \quad (1)$$

where

$$R_{\text{A}} = \delta(\mathcal{M}_{\infty}) \frac{2GM}{v_{\infty}^2} \quad (2)$$

is the accretion radius and

$$\delta(\mathcal{M}_{\infty}) = \left(\frac{\mathcal{M}_{\infty}^2}{1 + \mathcal{M}_{\infty}^2} \right)^{3/4}, \quad (3)$$

where $\mathcal{M}_{\infty} = v_{\infty}/c_{s,\infty}$ is the Mach number (Shima et al. 1985). The mean angular momentum of accreted matter is zero.

The in-spiral problem is more complicated due to the density and velocity gradients across the direction of motion of the NS. Provided the gradients are small on the scale of the accretion radius, the above expression for \dot{M} is still quite accurate (Ishii et al. 1993; Ruffert 1997, 1999). However, the accreted matter can now have a non-vanishing mean angular momentum. This was first suggested by Illarionov & Sunyaev (1975) in connection with X-ray binaries, where the accretion disc of the BH is fed by the stellar wind of the primary. Taking into account only the velocity gradients related to the orbital motion, they found that the mean specific angular momentum of accreted matter inside the accretion cylinder is

$$\langle j_{\text{A}} \rangle = \frac{1}{4} \Omega R_{\text{A}}^2, \quad (4)$$

where Ω is the angular velocity of the orbital motion. Shapiro & Lightman (1976) took into account the density gradient of the wind as well and refined this result,

$$\langle j_{\text{A}} \rangle = -\frac{1}{2} \Omega R_{\text{A}}^2, \quad (5)$$

where the minus sign shows that the disc rotation is now in the opposite sense to the orbital motion. Later, Davies & Pringle (1980) criticized the approach used by the previous authors. They generalized the original calculations of Hoyle & Lyttleton (1939) to include the density and velocity gradients and concluded that to the first order in R_{A}/h , where h is the length-scale of the variations, $\langle j_{\text{A}} \rangle = 0$. The 2D numerical simulations of Ishii et al. (1993) seemed to agree with this conclusion, whereas their 3D simulations still indicated the net accretion of angular momentum. Ruffert (1997, 1999) carried out an extensive 3D numerical investigation of the problem. Introducing an angle-dependent accretion radius, he also derived another version of the analytic expression for $\langle j_{\text{A}} \rangle$

$$\langle j_{\text{A}} \rangle = \frac{1}{4} (6\epsilon_v + \epsilon_{\rho}) v_0 R_{\text{A}}, \quad (6)$$

where

$$\epsilon_{\rho} = \frac{R_{\text{A}}}{\rho} \frac{d\rho}{dx} \quad \text{and} \quad \epsilon_v = \frac{R_{\text{A}}}{v} \frac{dv}{dx} \quad (7)$$

are the dimensionless gradients of density and velocity, respectively, with x being the transverse Cartesian coordinate. However, the numerical results did not agree with this expression, with $\langle j_{\text{A}} \rangle$ varying between 7 and 70 per cent of what is available in the accretion cylinder. Moreover, in the simulations, only the cases with either the velocity or the density gradient were considered, whereas in the in-spiral problem both are present. Although the computational resources and numerical algorithms have improved since 1999, no further attack on this problem has been attempted yet and the issue of $\langle j_{\text{A}} \rangle$ remains open.

For the in-spiral problem $v_0 = \Omega a$, $v(x) = v_0 + \Omega x$ and $\epsilon_v = R_{\text{A}}/a$, where a is the orbital radius of a NS. Assuming a power law

for the density distribution inside the RSG, $\rho \propto r^{-n}$, we also find $\epsilon_{\rho} = -nR_{\text{A}}/a$. This allows us to write equation (6) as

$$\langle j_{\text{A}} \rangle = \frac{1}{4} (6 - n) \Omega R_{\text{A}}^2, \quad (8)$$

which has the same dependence on Ω and R_{A} as in equations (4) and (5). Given the unsettled nature of this issue, we will assume that

$$\langle j_{\text{A}} \rangle = \frac{\eta}{4} \Omega R_{\text{A}}^2, \quad (9)$$

where η is a free parameter, which reflects our current ignorance.

In our case, M is the mass of the NS and v_{∞} is its orbital speed. Assuming that the interaction does not disturb the RSG inside the orbit, we have

$$v^2 \simeq \frac{GM_{*}}{a}, \quad (10)$$

where a is the orbital radius and M_{*} is the mass of the RSG inside the orbit. Under the same assumption, ρ_{∞} and $c_{s,\infty}$ can be replaced with the density and sound speed of the undisturbed RSG at radius $r = a$. The motion of the NS inside the RSG is only mildly supersonic, $\mathcal{M} \simeq 1.4$ (Chevalier 1993), allowing us to write

$$R_{\text{A}} \approx 2\beta \frac{aM_{\text{NS}}}{M_{*}}, \quad (11)$$

where $\beta \simeq 0.8$ and only weakly depends on the model of the RSG.

Given the specific angular momentum, we can estimate the distance from the NS at which the Bondi–Hoyle trapped gas will form an accretion disc as

$$R_{\text{c}} = \frac{\langle j_{\text{A}} \rangle^2}{GM_{\text{NS}}} \approx a\eta^2 \beta^4 \left(\frac{M_{\text{NS}}}{M_{*}} \right)^3. \quad (12)$$

In the literature, this radius is often called the circularization radius. Since the NS is not a point mass, the accretion disc forms only if $R_{\text{c}} > R_{\text{NS}}$. When this condition is satisfied, the recycling of the NS proceeds at the highest rate.

For $R \gg R_{\text{c}}$, the accretion on the NS may proceed in more or less spherical fashion and is well described by the Bondi solution, in which the accretion flow becomes supersonic at $R_{\text{acc}} = 0.25R_{\text{A}}$ (for the polytropic index $\gamma = 4/3$). Its collision with the NS and/or its accretion disc creates a shock wave which re-heats the flow. This will have no effect on the mass accretion rate only if the following two conditions are satisfied (Chevalier 1996).

First, the radiation produced by the gas heated at the accretion shock should not be able to escape beyond R_{A} . If it does, then the mass accretion rate is limited by the Eddington value

$$\dot{M}_{\text{Edd}} \sim 3 \times 10^{-8} M_{\odot} \text{ yr}^{-1}.$$

This condition is satisfied when the accretion shock radius

$$R_{\text{sh}} \approx 3 \times 10^9 R_{\text{c},6}^{1.48} \dot{M}_0^{-0.37} \text{ cm} \quad (13)$$

is smaller compared with the radiation trapping radius

$$R_{\text{tr}} \approx 3.4 \times 10^{13} \dot{M}_0 \text{ cm}. \quad (14)$$

For this to occur, \dot{M}_{BH} has to exceed the critical value

$$\dot{M}_{\text{cn1}} \approx 1.1 \times 10^{-3} R_{\text{c},6}^{1.08} M_{\odot} \text{ yr}^{-1} \quad (15)$$

(Chevalier 1996). This result was derived assuming that $R_{\text{c}} > R_{\text{NS}}$ and ignoring the General Relativity corrections.

Secondly, the shock has to be inside the sonic surface of the Bondi flow.¹ Otherwise, this shock cannot be a part of the stationary

¹ The shock radius in equation (13) is obtained assuming a cold supersonic flow at infinity

solution and hence the Bondi-type accretion cannot be realized. This condition is satisfied when \dot{M}_{BH} exceeds the critical value

$$\dot{M}_{\text{cn2}} \approx 10^4 R_{\text{acc},8}^{-2.7} R_{\text{c},6}^4 M_{\odot} \text{yr}^{-1} \quad (16)$$

(Chevalier 1996). As we shall see, this condition is more restrictive.

A note of caution has to be made at this point. The analytical expression for the accretion shock radius (13) is based on a number of assumptions and simplifications and its accuracy has not yet been tested via numerical simulations. At the moment, this can only be considered as an order of the magnitude estimate. When R_{c} becomes as small as the NS radius, this expression gives R_{sh} which exceeds the value given by the more reliable spherically symmetric model of Houck & Chevalier (1991) by a factor of 10 (see equations 13 and 23). Two reasons explain this disagreement. First, in the spherically symmetric models, the gravity is relativistic, whereas in the models with rotation, it is Newtonian. Secondly, the models use different assumptions on the geometry of the neutrino cooling region. It appears that equation (13) becomes increasingly less accurate when R_{c} approaches R_{NS} , overestimating R_{sh} . As a result, equation (16) overestimates the value of \dot{M}_{cn2} . We also note that the critical rates are quite sensitive to the parameter η ,

$$\dot{M}_{\text{cn1}} \propto \eta^{2.16} \quad \text{and} \quad \dot{M}_{\text{cn2}} \propto \eta^8.$$

In this study, we have considered six different models of the RSG. In the first two models, we assumed that the mass distribution in the stellar envelope is the power law $\rho \propto r^{-n}$ with $n = 2$ (model RSG2) and $n = 3$ (model RSG3). In both these models, the total stellar mass $M_* = 25 M_{\odot}$, the helium core mass $M_{\text{c}} = 1/3 M_*$, and the inner and the outer radii of the power-law envelope are 7×10^9 and 7×10^{13} cm, respectively. For these models, all calculations can be made analytically. This not only helps to develop a feel for the problem, but also provides useful test cases for numerical subroutines. The next two models are based on stellar evolution calculations and describe the RSG in the middle of the He-burning phase (Woosley, Heger & Weaver 2002; Heger et al. 2004). Their zero-age main-sequence (ZAMS) masses are $M = 20 M_{\odot}$ (model RSG20He) and $M = 25 M_{\odot}$ (model RSG25He). These data were kindly provided to us by Alexander Heger. The last two models, RSG20 and RSG25, describe a pre-supernova RSG with the same ZAMS masses.² They have very extended envelopes, increasing the chance of a CE phase.

Fig. 1 shows the Bondi–Hoyle and the critical accretion rates for these six models and the two extreme values of the parameter η , representing the cases of both very efficient ($\eta = 1$) and rather inefficient ($\eta = 0.1$) accretion of angular momentum (see equation 9). One can see that the condition of radiation trapping is not very restrictive. For $\eta = 1$ it is satisfied for $R < 3 \times 10^{11}$ cm in models RSG20 and RSG25, for $R < 3 \times 10^{12}$ cm in models RSG20He and RSG25He, and much earlier for $\eta = 0.1$.

On the contrary, the condition $\dot{M}_{\text{BH}} > \dot{M}_{\text{cn2}}$ can be quite restrictive. In fact, it is never satisfied when $\eta = 1$. In this case, the circularization radius is always too far away from the NS and the neutrino cooling is not efficient enough. For $\eta = 0.1$, the results seem more promising as this condition is satisfied long way before the NS merges with the core. For RSGs in the middle of the He-burning phase, this occurs almost at the same point where the radiation becomes trapped and a bit later for the pre-supernova RSGs. Thus, for $\eta = 0.1$, the NS already begins to hyperaccrete inside the

envelope of the RSG primary. However, for such a small value of η , the accretion disc becomes very compact and may even disappear, in which case the recycling efficiency is reduced.

Fig. 2 shows all the characteristic radii of the in-spiral problem for $\eta = 0.1$. One can see that for models RSG20 and RSG25, the disc accretion domain has $a > 3 \times 10^{10}$ cm. For model RSG20He, this domain includes the whole stellar envelope and for model RSG25He it splits into two zones. What is most important is that in all models the accretion begins to proceed with the Bondi–Hoyle rate while still in the disc regime.

Once the accretion disc is formed, the specific angular momentum of the gas settling on the NS surface is that of the last Keplerian orbit. In this case, the star will reach the rotational rate Ω after accumulating

$$\Delta M \approx \frac{\Omega I}{j_{\text{K}}} \approx 0.18 M_0 R_{\text{NS},6}^2 P_{-3} M_{\odot}, \quad (17)$$

where $I \approx (2/5) M R_{\text{NS}}^2$ is the final moment of inertia of the NS and j_{K} is the Keplerian angular momentum at the NS radius. Obviously, the same mass is required to recycle the observed millisecond pulsars in low-mass binaries and this allows us to conclude that the NS may well reach the gravitationally unstable rotation rate before collapsing into a BH.

When the accretion proceeds at the Bondi–Hoyle rate, the NS mass and orbit are related approximately as

$$\frac{a_{\text{end}}}{a_{\text{init}}} = \left(\frac{M_{\text{init}}}{M_{\text{end}}} \right)^{\sigma}, \quad (18)$$

where $\sigma = -M\dot{a}/\dot{M}a$. Chevalier (1993) found that for a $10 M_{\odot}$ RSG σ varies slowly between 5 and 7. According to these results, the NS increases its mass by $0.2 M_{\odot}$ after its orbital radius decreases by only a factor of few. This shows that the ‘window of opportunity’, where the disc accretion can proceed at the Bondi–Hoyle rate, does not have to be particularly wide. In order to obtain a more accurate estimate, one could integrate the evolution equation

$$\frac{\dot{a}}{a} = -\frac{4\pi G^2 M \rho}{v^3} \left[\frac{M}{M_*(1 + \mathcal{M}^{-2})^{3/2}} + \zeta C_{\text{D}} \right] \left(\zeta + 3 \frac{\rho}{\bar{\rho}} \right)^{-1}, \quad (19)$$

where $\bar{\rho}$ is the average density of the primary inside $r = a$, $C_{\text{D}} \approx 6.5$ is the drag coefficient (Shima et al. 1985) and $\zeta = 1 + M_{\text{N}}/M_*$ (Chevalier 1993). Figs 3 and 4 show the results of such integration for models RSG20, RSG25 and RSG25He, assuming that the hyperaccretion regime begins near the stellar surface and at $a = 3 \times 10^{10}$ cm, respectively. One can see that in all these cases the gravitationally unstable rotation rate is reached when a decreases by less than a factor of 5, in good agreement with the original estimate.

For $\eta = 1$, the mass accretion rate is low and the NS cannot spin up significantly inside the CE. What occurs in this case depends on the details of CE evolution. The CE can either be ejected leaving behind a close NS–WR binary or survive, leading to a merger of the NS and the RSG core (Taam & Sandquist 2000). The configuration after the merger is similar to that of the Thorne–Zydkow object (Thorne & Zytkow 1977; Barkov, Bisnovaty-Kogan & Lamzin 2001). The common view is that such objects cannot exist because the effective neutrino cooling leads to hyperaccretion and prompt collapse of the NS into a BH. This conclusion is based on the spherically symmetric model, where the circularization radius is zero and the flow stagnation surface coincides with the surface of the NS. However, during the in-spiral the orbital angular momentum of the NS is converted into the spin of the primary. Thus, one would expect the core to be tidally disrupted and form a massive accretion

² These models can be downloaded from the website <http://homepages.spa.umn.edu/~alex/stellarevolution/>.

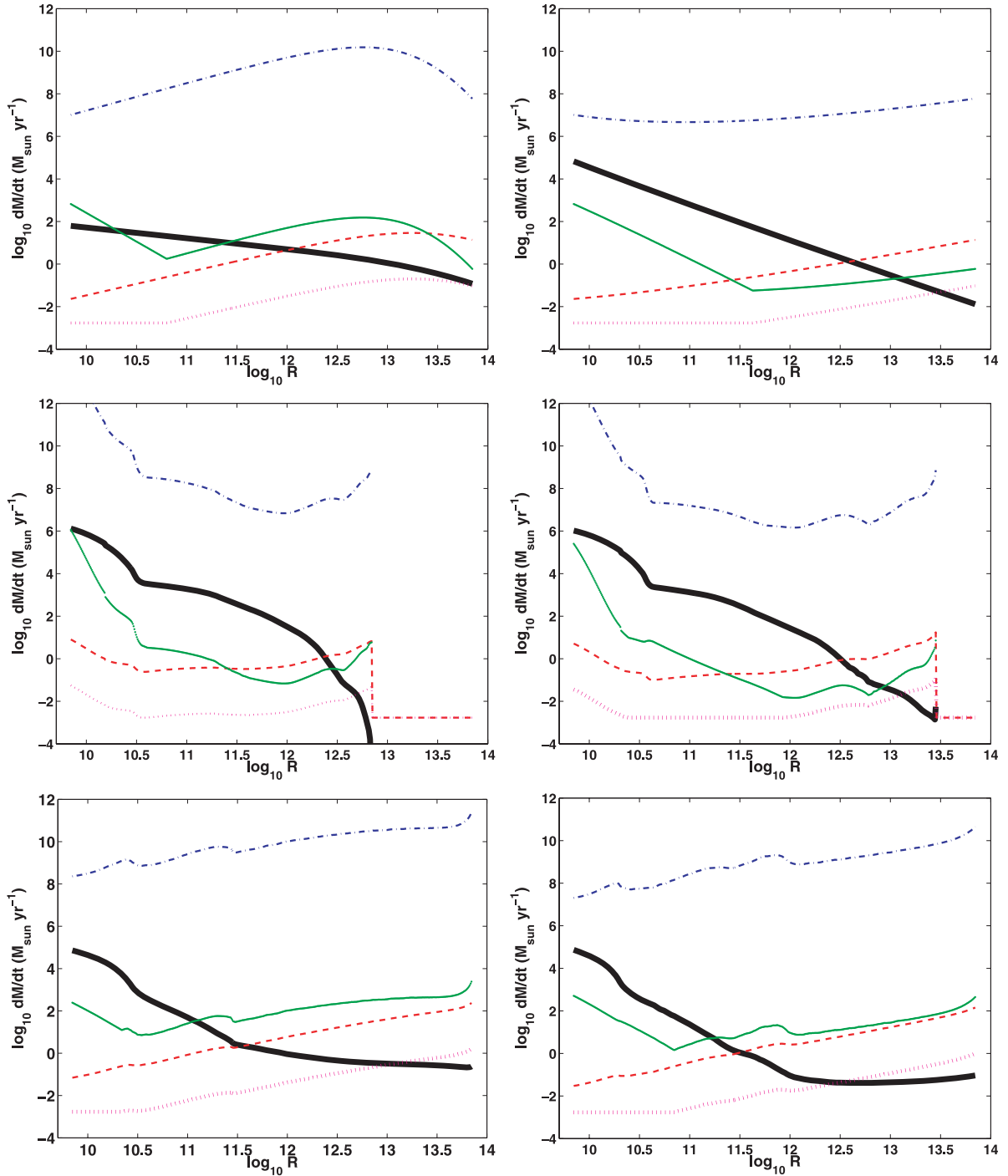


Figure 1. Accretion rate as a function of the position inside the RSG primary for six different models: RSG2 (left-hand top panel), RSG3 (right-hand top panel), RSG20He (left-hand middle panel), RSG25He (right-hand middle panel), RSG20 (left-hand bottom panel) and RSG25 (right-hand bottom panel). The Bondi–Hoyle rate, \dot{M}_{B-H} , is shown by the thick solid lines, the critical value \dot{M}_{cn1} is shown by the dotted ($\eta = 0.1$) and dashed ($\eta = 1$) lines, and the critical value \dot{M}_{cn2} is shown by the thin solid ($\eta = 0.1$) and dot–dashed ($\eta = 1$) lines.

disc around the NS. As a result, the cooling rate will be lower compared with that found in the spherically symmetric case. It is not obvious for how long this configuration may exist. However, this again opens the possibility of the recycling of the NS up to the gravitationally unstable rotation rate and magnetically driven stellar explosion.

In the case of core collapse, even the magnetic field of magnetar strength cannot prevent accretion and fails to drive the stellar

explosion (Komissarov & Barkov 2007). The magnetosphere becomes locked under the pile of accreting matter and a separated mechanism, for example, the standard neutrino-driven explosion, is required to release it. However, the density around the Fe core of pre-supernovae is very high, leading to very high accretion rates. In our case, the accretion rates are expected to be significantly lower. In the next section, we explore if they are low enough to allow purely magnetically driven explosions.

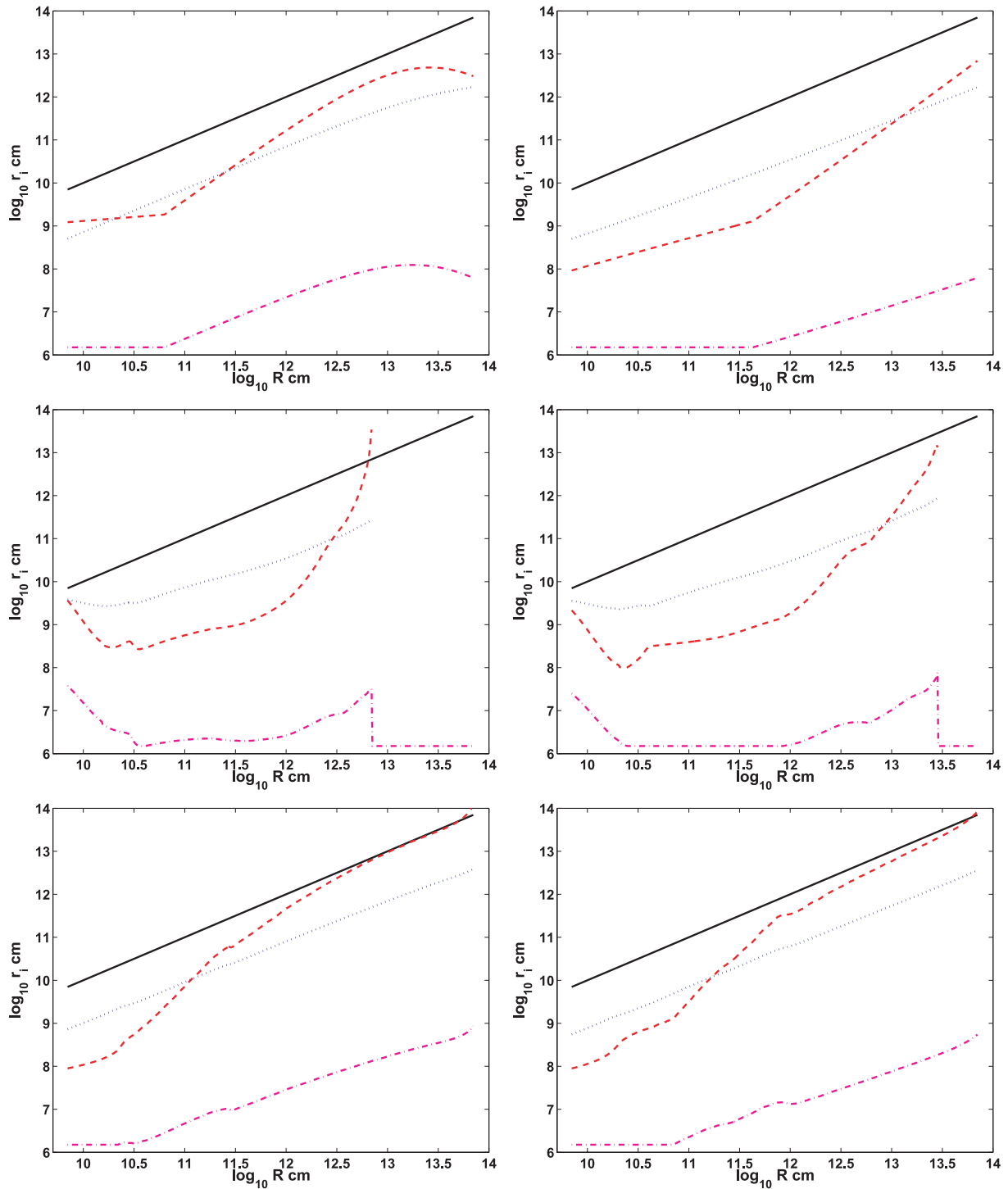


Figure 2. The characteristic radii of the in-spiral problem as functions of the position inside the RSG primary for the same models as in Fig. 1 and $\eta = 0.1$. The orbital radius is shown by the solid line, the sonic point, R_{acc} , is shown by the dotted line, the accretion shock radius is shown by the dashed line and the circularization radius, R_c , is shown by the dot-dashed line.

3 MAGNETIC EXPLOSION

3.1 Magnetic field generation

The main route to the formation of ‘magnetars’ is believed to be the core collapse of rapidly rotating stars. During the collapse, the proto-NS naturally develops strong differential rotation, with the

angular velocity decreasing outwards. This allows the generation of super-strong magnetic field via the α - Ω dynamo (Duncan & Thompson 1992; Thompson & Duncan 1993) or magnetorotational instability (Burrows et al. 2007).

In our case, the conditions are rather different. The NS is already fully developed, with a solid crust, when it enters the envelope of its companion. The typical NS crust has the thickness $h \approx 10^5$ cm

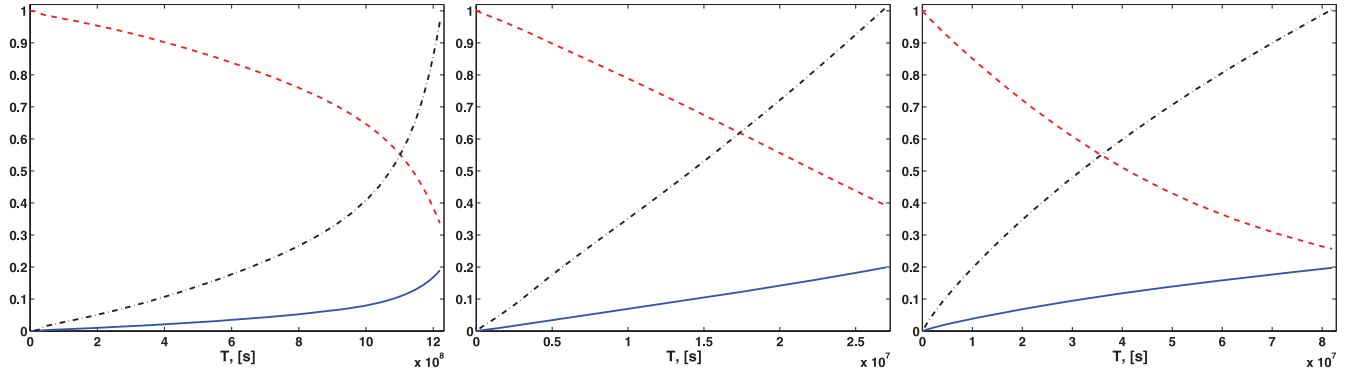


Figure 3. Evolution of the NS in the case when the Bondi–Hoyle regime begins at the surface of the RSG primary for models RSG25He (left-hand panel), RSG20 (middle panel) and RSG25 (right-hand panel). The lines show the accreted mass normalized to M_{\odot} (solid line), the angular momentum of the NS normalized to the critical value $j_c = I\Omega_c$, where $\Omega_c = 760$ Hz (dot-dashed line), and the orbital radius normalized to its initial value (dashed line).

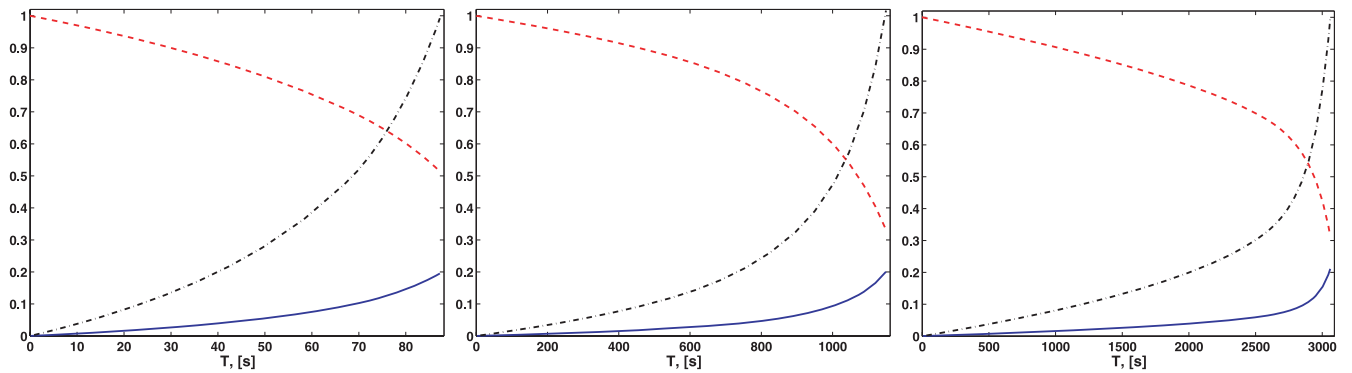


Figure 4. The same as in Fig. 3, but for the case when the Bondi–Hoyle regime starts at $a = 3 \times 10^{10}$ cm.

and the density at the bottom $\rho \sim 10^{14} \text{ g cm}^{-3}$ (see e.g. Gnedin, Yakovlev & Potekhin 2001; Lattimer & Prakash 2007). The NS may have already been spun up via the accretion from the stellar wind, but its rotation rate may still be well below the critical for the development of the gravitational wave instability. In any case, the accreted gas of the companion’s envelope forms a very rapidly rotating layer above the crust. As long as the crust exists, this layer and the NS core are basically decoupled and interact mainly gravitationally. A strong tangential discontinuity exists at the outer boundary of the crust (Inogamov & Sunyaev 1999, 2010).

As the mass of the outer layer increases, the crust pressure goes up. Because of the degeneracy of the crust matter, its pressure depends mainly on its density, and only weakly on the temperature. When the density reaches the critical value $\rho_{\text{cr}} \sim 10^{14} \text{ g cm}^{-3}$, the crust begins to melt down (Brown 2000), and the barrier separating the NS core and its outer rotating layer disappears. If we ignore the centrifugal force, then this occurs when the NS accumulates mass comparable to the crust mass, $\sim 0.05 M_{\odot}$. The centrifugal force significantly reduces the effective gravitation acceleration and the above estimate for the layer mass is only a lower limit. Assuming $v_{\phi} \approx v_K \sim 10^{10} \text{ cm s}^{-1}$, the rotational energy of the layer at the time of melting may well reach $\sim 10^{52}$ erg. Once the crust has melted, the core and the layer can begin to interact hydromagnetically, with up to $E \sim 10^{52}$ erg of energy in differential rotation to be utilized.

One possibility is viscous heating and neutrino emission. We can estimate the neutrino luminosity as $L_{\nu} \approx E/t_d$, where t_d is

the neutrino diffusion time. Following the analysis of Lattimer & Prakash (2007) and Barkov (2008), this time can be estimated as

$$t_d \sim \frac{h\tau_{\nu}}{c}, \quad (20)$$

where $\tau_{\nu} = h\rho\Sigma_{\nu}/m_p$ is the optical depth of the hot envelope for the neutrino emission. Assuming equilibrium with the electron fraction $Y_e = 0.05$, the mean neutrino cross-section is about $\Sigma_{\nu} \approx \sigma_{\nu}\epsilon_{\nu}kT_e/m_e^2c^4$, where $\sigma_{\nu} = 1.7 \times 10^{-44} \text{ cm}^2$ (Bahcall 1964) and $\epsilon_{\nu} \approx 3.15kT_e$ is the mean energy of the neutrino (Thompson, Burrows & Meyer 2001). The temperature can be estimated as

$$T_e \approx \left(\frac{E}{4\pi a_r h R_{\text{NS}}^2} \right)^{1/4} \approx 10^{12} E_5^{1/4} h_5^{-1/4} R_{\text{NS},6}^{-1/2} \text{ K},$$

where $a_r = 7.564 \times 10^{-15} \text{ erg cm}^{-3} \text{ K}^{-4}$ is the radiation constant. The corresponding diffusion time is quite short,

$$t_d \sim \frac{0.1 h_5^{3/2} \rho_{14} E_{52}^{1/2}}{R_{\text{NS},6}} \text{ s}.$$

Another process is the development of the Kelvin–Helmholtz instability, the production of the turbulence and amplification of magnetic field. For the Kelvin–Helmholtz instability to develop, the Richardson number J has to be less than 1/4 (Chandrasekhar 1961). In our case

$$J \approx \frac{gh}{v_{\phi}^2} \approx 0.2 R_{\text{NS},6} h_5, \quad (21)$$

where $g \approx GM_{\text{NS}}/R_{\text{NS}}^2$ is the gravitational acceleration and we use $M_{\text{NS}} = 1.5M_{\odot}$. Thus, the instability condition is marginally satisfied. Once the turbulence has developed, the magnetic field amplification is expected to proceed as discussed in Duncan & Thompson (1992). The e-folding time is given by the eddy turnover time, which one would expect to be below the rotation period of the outer layer. Thus, strong magnetic field can be generated on the time below the viscous and the neutrino diffusion time-scale.³ This conclusion is supported by the recent numerical simulations of similar problems, which show that the time as short as 0.03 s can be sufficient to generate dynamically strong magnetic field (Obergaullinger et al. 2009; Rezzolla et al. 2011). The strong toroidal magnetic field can suppress the instability if $\rho v^2 < B^2/4\pi$ (Chandrasekhar 1961) or if $B > 3 \times 10^{17}$ G. This is likely to determine the saturation strength of magnetic field. Such a strong magnetic field is also buoyant (Spruit 1999) and will emerge from under the NS surface into the surrounding accretion flow.

Another possibility of generating super-strong magnetic field in the recycled NS was proposed by Spruit (1999) with an application to X-ray binaries. In this model, the NS spins up to the critical rotation rate where it becomes unstable to exciting r modes and gravitational radiation (Levin 1999; Spruit 1999). This may lead to effective braking of the outer layers of the NS and developing strong differential rotation. Recent studies, however, suggest that non-linear coupling with other modes leads to the saturation of the r mode at a much lower amplitude (Arras et al. 2003; Brink et al. 2005; Bondarescu et al. 2007), though the mass accretion rates assumed in these studies are much lower than those encountered in CE.s.

3.2 Criteria for explosions

Depending on the mass accretion rate, this may just modify the properties of the accretion flow near the star, the ‘accretor’ regime, or drive an outflow (e.g. Illarionov & Sunyaev 1975). In the latter case, two different regimes are normally discussed in the literature, the ‘propeller’ regime and the ‘ejector’ regime. In the ejector regime, the magnetosphere expands beyond the light cylinder and develops a pulsar wind. In the propeller regime, the magnetosphere remains confined to the light cylinder. If the magnetic axis is not aligned with the rotational axis, then the magnetosphere may act in a similar fashion to an aircraft propeller, driving shock waves into the surrounding gas, heating it and spinning it up. If the energy supplied by the propeller is efficiently radiated away, this may lead to a quasi-static configuration (e.g. Mineshige, Rees & Fabian 1991). If not, the most likely outcome is an outflow, followed by the expansion of the magnetosphere, and the transition to the ejector regime.

This classification is applied both in the case of quasi-spherical accretion and in the case of disc accretion. In the disc case, the external gas above and below the disc is usually not considered as important dynamical element. However, in our case, this is not true because the accretion disc is rather compact and feeds from a more or less spherical component of the accretion flow. If the expanding magnetosphere removes this component, the disc will no longer be supplied with mass and quickly disappear, no matter what its regime is. For this reason, we will not consider the complicated

interaction between the magnetosphere and the disc,⁴ but will focus on the interaction with the low angular momentum flow of the polar regions which accretes directly on to the NS avoiding the disc. In order to simplify the problem, we will treat this flow as spherically symmetric, keeping in mind that its mass accretion rate is only a fraction of the Bondi–Hoyle rate.

The extent of the magnetosphere is often estimated by the balance between the magnetic pressure and the ram pressure of accreting flow. This is fine when the accretion shock is close to the NS. If not, the thermal pressure at the magnetospheric radius can be significantly higher compared both to the actual ram pressure at the shock and to the ram pressure that would be found at the magnetospheric radius if the free-fall flow could continue down to this radius. In this case, the initial radius of the emerging magnetosphere is rather determined by the balance of the magnetic pressure and the thermal pressure of the quasi-hydrostatic ‘settling’ flow downstream of the accretion shock (Mineshige et al. 1991).

Assuming that the accretion flow in the polar region is approximately spherical, we can describe it using the analytical model developed by Houck & Chevalier (1991). Repeating their calculations with the more accurate cooling function, adopted later in Chevalier (1996),

$$\dot{\epsilon}_{\text{n}} = 10^{25} \left(\frac{kT}{\text{MeV}} \right)^9 \text{ erg cm}^{-3} \text{ s}^{-1} \quad (22)$$

(Dicus 1972; Brown & Weingartner 1994) and using the adiabatic index $\gamma = 4/3$, we find the accretion shock radius

$$R_{\text{sh}} \simeq 8.2 \times 10^8 f_1 R_{\text{NS},6}^{40/27} M_0^{-1/27} \dot{M}_0^{-10/27} \text{ cm}, \quad (23)$$

where

$$f_1 = \left\{ \frac{R_{\text{NS}}}{R_{\text{g}}} \left[\left(1 - \frac{2R_{\text{g}}}{R_{\text{NS}}} \right)^{-1/2} - 1 \right] \right\}^{-64/27} \quad (24)$$

and $R_{\text{g}} = GM/c^2$ is the gravitational radius of the NS. (In the calculations, we assume the Schwarzschild space–time.) For reasonable masses and radii of NSs, $0.27 < f_1 < 0.62$. In particular $f_1 = 0.54$ for $M = M_{\odot}$ and $R_{\text{NS}} = 10$ km. Downstream of the shock we have an adiabatic subsonic flow with the mass density

$$\rho = \rho_{\text{sh}} \left(\frac{R}{R_{\text{sh}}} \right)^{-3}, \quad (25)$$

where

$$\rho_{\text{sh}} = \frac{7}{4\pi} \frac{\dot{M}}{(GM)^{1/2} R_{\text{sh}}^{3/2}} \quad (26)$$

is the mass density at the shock, the pressure

$$p = \frac{6}{7} p_{\text{ram}}(R_{\text{sh}}) \left(\frac{R}{R_{\text{sh}}} \right)^{-4}, \quad (27)$$

where

$$p_{\text{ram}}(R_{\text{sh}}) = \frac{\dot{M} \sqrt{GM}}{4\pi R_{\text{sh}}^{5/2}} \quad (28)$$

is the ram pressure of the free-falling flow at the shock, the temperature

$$T = \left(\frac{12}{11a} p \right)^{1/4}, \quad (29)$$

³ The viscous dissipation time-scale is very long $t_{\text{vis}} \approx 10^8 R_{\text{NS},6}^{23/4} T_9^2$ s (Shapiro 2000).

⁴ An interested reader may find out more about the disc–magnetosphere interaction from Ustyugova et al. (2006) and references therein.

where a is the radiation constant, and the radial component of 4-velocity

$$u = -\frac{\dot{M}}{4\pi\rho R^2}. \quad (30)$$

Assuming that the magnetosphere expands until its magnetic pressure equals the gas pressure,⁵ we find the radius of the dipolar magnetosphere with the surface strength B_{NS} to be

$$R_m = 5 \times 10^6 f_1^{-3/4} R_{\text{NS},6}^{17/9} M_0^{-2/9} \dot{M}_0^{-2/9} B_{\text{NS},15} \text{ cm}. \quad (31)$$

For this to be above the NS radius, the mass accretion rate should not exceed

$$\dot{M}_{\text{cr}} \simeq 1.3 \times 10^3 f_1^{-27/8} B_{\text{NS},15}^{9/2} R_{\text{NS},6}^4 M_0^{-1} M_{\odot} \text{ yr}^{-1}. \quad (32)$$

The traditional criterion for the propeller regime is that the magnetospheric radius is below the light cylinder radius

$$R_{\text{LC}} = \frac{cP}{2\pi} \simeq 4.8 \times 10^6 P_{-3} \text{ cm} \quad (33)$$

and above the corotation radius

$$R_{\text{cor}} = \left(\frac{GM}{\Omega^2}\right)^{1/3} \simeq 1.5 \times 10^6 P_{-3}^{2/3} M_0^{1/3} R_{\text{NS},6} \text{ cm}, \quad (34)$$

at which the magnetosphere rotates with the local Keplerian velocity.

The ejector regime is realized when $R_m > R_c$. In terms of the mass accretion rate, the propeller regime criterion can be written as

$$\dot{M}_{\text{ej}} < \dot{M} < \dot{M}_{\text{pr}}$$

and the ejector regime criterion as

$$\dot{M} < \dot{M}_{\text{ej}},$$

where

$$\dot{M}_{\text{pr}} \simeq 2 \times 10^2 f_1^{-27/8} M_0^{-5/2} R_{\text{NS},6}^{17/2} B_{\text{NS},15}^{9/2} P_{-3}^{-3} M_{\odot} \text{ yr}^{-1} \quad (35)$$

and

$$\dot{M}_{\text{ej}} \simeq 1.1 f_1^{-27/8} M_0^{-1} R_{\text{NS},6}^{17/2} B_{\text{NS},15}^{9/2} P_{-3}^{-9/2} M_{\odot} \text{ yr}^{-1}. \quad (36)$$

The latter is much stronger and even if only a fraction of the total mass accretion rate is shared by the quasi-spherical component, it could be satisfied only during the early phase of the in-spiral (see Fig. 1). More likely, the emerged magnetosphere will operate in the propeller regime.

The sound speed in the Houck & Chevalier (1991) solution depends only of the NS mass and the distance from the NS,

$$c_s \simeq 6.2 \times 10^9 M_0^{1/2} R_6^{-1/2} \text{ cm s}^{-1}. \quad (37)$$

The linear rotational velocity of the magnetosphere,

$$v_{\text{rot}} \simeq 4.8 \times 10^9 P_{-3}^{-1} R_6 \text{ cm s}^{-1}, \quad (38)$$

is generally higher and thus we have the so-called supersonic propeller. The power generated by such a propeller is roughly

$$\begin{aligned} L_{\text{pr}} &\simeq \frac{4\pi}{3} p_m R_m^2 \frac{(R_m \Omega)^2}{c_s} \\ &\simeq 1.3 \times 10^{50} f_1^{9/8} B_{\text{NS},15}^{1/2} P_{-3}^{-2} \dot{M}_0^{1/3} M_0^{1/6} \text{ erg s}^{-1} \end{aligned} \quad (39)$$

⁵ As a result of its oscillations, the NS can become quite hot and fill the magnetosphere with substantial amount of plasma. In this case, the centrifugal force will need to be included in the force balance, yielding an even higher value for R_m .

(Mineshige et al. 1991), exceeding by several orders of magnitude the accretion power

$$L_{\text{acc}} = \frac{GM\dot{M}}{R_{\text{NS}}} \simeq 8 \times 10^{45} M_0 R_{\text{NS},6}^{-1} \dot{M}_0 \text{ erg s}^{-1}. \quad (40)$$

This suggests that the magnetosphere easily blows away the accreting matter and expands beyond the light cylinder, thus creating the conditions for a proper pulsar wind from the NS.

One may argue that the accretion flow could re-adjust to the new conditions, with the accretion shock moving farther out, the temperature at the magnetospheric radius rising and the enhanced neutrino cooling compensating for the propeller heating, $L_n = L_{\text{pr}}$. (A similar problem has been analysed by Mineshige et al. 1991.) Given the strong dependence of the neutrino emissivity on the temperature, the cooling is expected to be significant only in the close vicinity of the magnetosphere. In the non-magnetic case, most of the cooling occurs in the volume comparable to the NS volume (Houck & Chevalier 1991). This suggests that in our case the cooling volume will be approximately the same as the volume of the magnetosphere. Then the energy balance can be written as

$$\frac{4\pi}{3} R_m^3 \dot{\epsilon}_n(T) = L_{\text{pr}}, \quad (41)$$

where $\dot{\epsilon}_n(T)$ is given by equation (22). Solving this equation for R_m , simultaneously with the pressure balance

$$p(R_m) = \frac{1}{8\pi} B_0^2 \left(\frac{R_m}{R_{\text{NS}}}\right)^{-6}, \quad (42)$$

where $p(R)$ is given by equation (27), we find that

$$\frac{R_m}{R_{\text{NS}}} \simeq 0.6 B_{\text{NS},15}^{5/18} R_{\text{NS},6}^{-1/6} M_0^{1/18} P_{-3}^{2/9}, \quad (43)$$

independently of the mass accretion rate. Since in this solution $R_m < R_{\text{NS}}$, we conclude that the accretion flow cannot re-adjust itself and will be terminated by the emerged magnetosphere.

In the case of cold NSs, the pulsar wind power

$$L_w \simeq \frac{\mu^2 \Omega^4}{c^3} (1 + \sin^2 \theta_m) \simeq 6 \times 10^{49} B_{\text{NS},15}^2 R_{\text{NS},6}^6 P_{-3}^{-4} \text{ erg s}^{-1}, \quad (44)$$

where $\mu = B_0 R_{\text{NS}}^2$ is the star magnetic moment and θ_m is the angle between the magnetic moment and the rotational axis of the NS (Spitkovsky 2006). For a hot NS, the mass loading of the wind can be substantial, leading to even higher luminosity (Bucciantini et al. 2006; Metzger, Thompson & Quataert 2007). The energy released in the magnetically driven explosion is the rotational energy of the NS

$$E_{\text{rot}} = \frac{1}{2} I \Omega^2 \simeq 1.6 \times 10^{52} M_0 R_{\text{NS},6}^2 P_{-3}^2 \text{ erg}, \quad (45)$$

where $I \simeq (2/5) M_{\text{NS}} R_{\text{NS}}^2$ is the NS moment of inertia.

Inside the RSG core, the accretion rate is expected to be much higher. For example, in model RSG20He, the core density $\rho \simeq 8.6 \times 10^2 \text{ g cm}^{-3}$ and the pressure $p \simeq 1.3 \times 10^{19} \text{ g cm}^2 \text{ s}^{-2}$, yielding the Bondi accretion rate

$$\dot{M}_{\text{B}} \simeq \pi \frac{(GM)^2 \rho}{c_s^3} \simeq 4.3 \times 10^5 M_{\odot} \text{ yr}^{-1}. \quad (46)$$

For such a high accretion rate, the propeller regime requires the magnetic field to be well in excess of 10^{15} G , similar to what is required in the magnetar models of GRBs. Whether such a strong dipolar magnetic field can be generated is not clear at present, as the observations of known magnetars suggest lower values. However, this could be a result of the short decay time expected for such a strong field (Heyl & Kulkarni 1998).

4 SUPERNOVA PROPERTIES

4.1 The plateau

Since the NS has to reach the maximum allowed rotation rate before it explodes, the model predicts the explosion energy around 10^{52} erg, putting it on the level of hypernovae. The corresponding ejecta speed will be very high

$$v_{\text{ej}} = 10^9 M_{\text{ej},1}^{-1/2} \text{ cm s}^{-1}, \quad (47)$$

where $M_{\text{ej},1}$ is the ejected mass.

Since the progenitor is a RSG, the supernova spectra will show hydrogen lines and would be classified as Type II. As the NS spirals through the weakly bound outer envelope of its RSG companion, it drives an outflow with the speed about the local escape speed and the mass-loss rate about $M_{\odot} \text{ yr}^{-1}$ (Taam & Sandquist 2000). The total in-spiral time is about few initial orbital periods. For a RSG with mass $20 M_{\odot}$ and their radius $R = 10^{14}$ cm, this yields $v_{\text{esc}} = 5 \times 10^6 \text{ cm s}^{-1}$ and $t_{\text{ins}} \sim \text{few} \times 10^8$ s. Thus, we expect a hydrogen-rich circumstellar shell of few solar masses to exist at a distance of $\sim 10^{15}$ cm at the time of the supernova explosion. The presence of such a shell will delay the transition to the adiabatic expansion phase and increase the supernova brightness similar to how this occurs in Type II_n supernovae (Chugai et al. 2004; Smith et al. 2007, 2008; Woosley, Blinnikov & Heger 2007).

Following Kasen & Bildsten (2010), the supernova luminosity during the phase of adiabatic expansion can be estimated as

$$L \simeq \frac{E_{\text{rot}} t_e}{t_d^2}, \quad (48)$$

where $t_e = R_0/v_{\text{ej}}$ is the expansion time-scale and R_0 is the progenitor radius, and

$$t_d = \left(\frac{3}{4\pi} \frac{M_{\text{ej}} k}{c v_{\text{ej}}} \right)^{1/2} \quad (49)$$

is the radiative diffusion time-scale and k is the opacity. (In the estimates below, we use $k = 0.4 \text{ cm}^2 \text{ g}^{-1}$, the value for Thomson scattering in the fully ionized plasma.) It is assumed that the initial magnetar spin-down time-scale is smaller compared to t_e , which is certainly satisfied in our case, given the large required magnetic field, 10^{15} – 10^{16} G. For the characteristic parameters of the model, we have

$$t_e \simeq 10^5 R_{0,14} v_{\text{ej},9}^{-1} \text{ s}, \quad t_d \simeq 8 \times 10^6 M_{\text{ej},1}^{1/2} v_{\text{ej},9}^{-1/2} \text{ s}, \quad (50)$$

and

$$L \simeq 1.6 \times 10^{43} R_{0,14} M_{\text{ej},1} \text{ erg s}^{-1}. \quad (51)$$

This high luminosity will be sustained for up to $t \sim t_d$, after which the trapped radiation, generated by the blast wave when it was crossing the star, escapes and the luminosity drops. In most normal Type II supernovae, the luminosity after this point is sustained via the radioactive decay of isotopes, mainly ^{56}Ni , produced by the supernova shock in the high-density environment around the collapsed core. However, in our model, the stellar structure is significantly different from that of normal pre-supernovae.

4.2 ^{56}Ni production

If the explosion occurs after the NS is settled into the centre of RSG20He, then the core density is only $\rho_c \simeq 8 \times 10^2 \text{ g cm}^{-3}$ and its temperature $T_c \simeq 1.9 \times 10^8 \text{ K}$, and $R_A = GM/c_s^2$ is the Bondi accretion radius.

As the magnetically driven explosion develops, a shock wave propagates through the body of the RSG. Where the post-shock temperature exceeds $T_{\text{Ni}} \simeq 10^9 \text{ K}$, ^{56}Ni is produced in abundance (Woosley et al. 2002). In order to capture the shock dynamics, we need to know the structure of the accretion flow on to the NS, which has been established before the explosion. This flow is rather complicated because of its rotation and without computer simulations we can only make very rough estimates.

First, consider the polar region where the flow is more of less spherically symmetric. Equation (13) shows that the accretion shock is quite close to the NS, particularly when it is near the RSG core, and hence most of the flow can be described using the free-fall model. The ram pressure of the accretion flow in this model is given by

$$\rho v_{\text{ff}}^2 = \frac{\dot{M} \sqrt{2GM}}{4\pi} R^{-5/2}, \quad (52)$$

where $v_{\text{ff}} = (2GM/R)^{1/2}$ is the free-fall speed. Close to the NS, the speed of the explosion shock, v_{sh} , is much less compared to v_{ff} and can be found from the pressure balance equation

$$\frac{2}{\gamma + 1} \rho v_{\text{ff}}^2 = \frac{E}{4\pi R^3}, \quad (53)$$

where R is the shock radius and $E = L_w t$ is the energy injected by the magnetar. This yields

$$t = \frac{2\dot{M} \sqrt{2GM}}{(\gamma + 1)L_w} R^{1/2} \quad (54)$$

and thus the shock speed increases with the distance. This approximation breaks down at the radius

$$R_t = \frac{2\dot{M}GM}{(\gamma + 1)L_w}, \quad (55)$$

where $v_{\text{sh}} = v_{\text{ff}}$. The gas temperature exceeds T_{Ni} inside the radius R_{Ni} determined by the equation

$$\frac{2}{\gamma + 1} \rho v_{\text{ff}}^2 = \frac{a}{3} T_{\text{Ni}}^4, \quad (56)$$

and the total mass of the produced ^{56}Ni can be estimated as

$$M_{\text{Ni}} = \dot{M} t_{\text{Ni}}, \quad (57)$$

where t_{Ni} is the time required for the shock to reach R_{Ni} according to equation (54). From equations (55–57), we find that

$$R_t = 10^8 \dot{M}_6 L_{w,50}^{-1} \text{ cm}, \quad (58)$$

$$R_{\text{Ni}} = 7.8 \times 10^7 \dot{M}_6^{2/5} \text{ cm}, \quad (59)$$

$$M_{\text{Ni}} = 0.003 \dot{M}_6^{11/5} L_{w,50}^{-1} M_{\odot}. \quad (60)$$

Thus, only a relatively small amount of ^{56}Ni can be produced even for the highest mass accretion rates allowed in this model.

In the equatorial plane, the accretion shock can be pushed all the way towards R_{acc} (see Section 2). Downstream of the shock, the flow is highly subsonic with

$$\rho = \rho_0 \left(\frac{R}{R_0} \right)^{-3}. \quad (61)$$

The highest density is achieved when the accretion shock is infinitely weak and this law is applied up to the sonic point R_{acc} . In this case, we can put $R_0 = R_{\text{acc}}$ and $\rho_0 = \rho_*$, the mass density of the RSG. The equation for shock speed is now

$$\frac{2}{\gamma + 1} \rho v^2 = \frac{E}{4\pi R^3}, \quad (62)$$

which yields the shock radius

$$R = \frac{2}{3} \left[\frac{(\gamma + 1)L_w}{8\pi\rho_* R_{\text{acc}}^3} \right]^{1/2} t^{1/2}. \quad (63)$$

R_{Ni} is now determined by the equation

$$\frac{2}{\gamma + 1} \rho v^2 = \frac{aT_{\text{Ni}}^4}{3}, \quad (64)$$

where the mass of the produced ^{56}Ni is still given by equation (57). Combining equations (63) and (64), we find

$$M_{\text{Ni}} \propto \dot{M} R_{\text{acc}}^{9/7} \rho_*^{3/7} L_w^{1/7}. \quad (65)$$

The highest values for M_{Ni} are obtained inside the RSG core. For model RSG20He, where $R_{\text{acc}} \sim 5 \times 10^9$ cm, $\dot{M} \sim 10^6 M_{\odot} \text{ yr}^{-1}$ (see Figs 1 and 2) and $\rho_* \sim 5 \times 10^2 \text{ g cm}^{-3}$, we find $M_{\text{Ni}} \simeq 0.02 M_{\odot}$. Although significantly higher, this is still small compared to the mass deduced from the observations of most supernovae.

If the density behind the shock wave is lower than 10^6 g cm^{-3} , which corresponds to $\dot{M} < 10^6 M_{\odot} \text{ yr}^{-1}$, then the photon dissociation of Ni^{56} becomes important as well (Magkotsios et al. 2010). Thus, our estimation gives only an upper limit to the amount of the produced Ni^{56} .

Another potential source of ^{56}Ni is the wind from the accretion disc itself, like in the collapsar model of a GRB. Without a robust disc model, it is difficult to figure out how effective this mechanism is. For example, in the numerical simulations of MacFadyen & Woosley (1999), the outcome was dependent on the rate of the introduced ‘viscous’ dissipation. In any case, the much lower accretion rates encountered in our model suggest that the amount of ^{56}Ni will be lower too. Thus, we conclude that our model predicts significant deficit of ^{56}Ni .

4.3 The long-term effects of the magnetar wind

It has been suggested recently that the long-term activity of magnetars born during the core collapse can power the supernova light curves, mimicking the effect of radioactive decay (Kasen & Bildsten 2010; Woosley 2010). In these studies, it was assumed that the rotational energy of the magnetar, released at the rate $\propto t^{-2}$, is converted into heat at the base of the supernova ejecta. One mechanism of such heating is purely hydrodynamical, via the forward shock wave involved in the collision of the fast magnetar wind with the slower supernova ejecta. In our case, however, this shock is the supernova shock and it is not present since the break-out. The other mechanism, heating by the radiation produced at the termination shock of the magnetar wind, remains in force and here we explore its efficiency.

Combining equations (44) and (45), it is easy to obtain the well-known law of the asymptotic spin-down of magnetic rotators

$$\Omega = \left(\frac{Ic^3}{2\mu^2 t} \right)^{1/2} \simeq 40 B_{\text{NS},15}^{-1} t_7^{-1/2} \text{ s}^{-1} \quad (66)$$

and

$$L_w = \frac{1}{4} \frac{I^2 c^3}{\mu^2 t^2} \simeq 10^{41} B_{\text{NS},15}^{-2} t_7^{-2} \text{ erg s}^{-1}. \quad (67)$$

(In this section, we use $R_{\text{NS}} = 10^6$ cm and $M_{\text{NS}} = 1.5 M_{\odot}$.) The last equation shows that unless $B < 10^{15}$ G the supernova luminosity will drop dramatically after the plateau phase. Such evolution has been observed in some supernovae, for example, SN 1994W (Tsvetkov 1995; Sollerman, Cumming & Lundqvist 1998).

In order to see how exactly this energy can be used to heat the supernova ejecta, we can appeal to the observed properties of pulsar

wind nebulae. For example, the study of the Crab nebula by Kennel & Coroniti (1984) indicates that immediately behind the termination shock most of the energy is in the form of ultrarelativistic electrons and only a fraction of it is in the magnetic field and there is no good reason to expect this to be different for magnetar winds. However, the magnetic field of a 1-yr-old magnetar wind nebula (MWN) is expected to be very strong, making the synchrotron cooling time very short.

One can estimate the magnetic field strength via the pressure balance at the termination shock

$$\frac{L_w}{4\pi R_w^2 c} = \frac{B^2}{8\pi}, \quad (68)$$

where R_w is the radius of the termination shock. Assuming that $R_w \simeq v_{\text{ej}} t$, this yields

$$B \simeq 0.3 t_7^{-2} B_{\text{NS},15}^{-1} v_{\text{ej},9}^{-1} \text{ G}. \quad (69)$$

The lowest energy electrons accelerated at the termination shock of the Crab nebula have the Lorentz factor $\gamma \sim 10^6$ (Kennel & Coroniti 1984). In the magnetic field of the MWN, they produce synchrotron photons with energy

$$E_v \simeq 100 B_{0,15}^{-1} v_{\text{ej},9}^{-3/2} t_7^{-2} \text{ keV} \quad (70)$$

and their synchrotron cooling time

$$t_{\text{syn}} \simeq 10^4 t_7^4 B_{\text{NS},15}^2 v_{\text{ej},9}^2 \text{ s} \quad (71)$$

is shorter compared to the dynamical time-scale for few years after the explosion.

The observations of the Crab nebula also show that the electrons are accelerated up to the radiation reaction limit (de Jager et al. 1996; Komissarov & Lyutikov 2011). Assuming that the same is true in our case, we expect the synchrotron spectrum to continue up to $E_{v,\text{syn}}^{\text{max}} \approx 100$ MeV and the highest energy of the electrons to be

$$E_e^{\text{max}} \simeq 100 t_7 B_{\text{NS},15}^{1/2} v_{\text{ej},9}^{1/2} \text{ TeV}. \quad (72)$$

These electrons also cool via the IC scattering on the soft photons produced by the supernova shell. The ratio of the IC to the synchrotron energy losses $\xi = u_{\text{soft}}/u_B$, where u_{soft} is the energy density of the soft radiation and $u_B = B^2/8\pi$ is the magnetic energy density. During the plateau phase

$$u_{\text{soft}} \simeq \frac{L_{\text{soft}}}{4\pi R_{\text{ph}}^2 c}, \quad (73)$$

where R_{ph} is the radius of the photosphere. Combining this result with equation (68), we find

$$\xi \simeq \frac{L_{\text{soft}}}{L_w} \left(\frac{R_w}{R_{\text{ph}}} \right)^2. \quad (74)$$

As we have seen, L_{soft} can be much higher than L_w but, on the other hand, R_w can be much lower than R_{ph} . Thus, it is hard to tell whether the IC emission can compete with the synchrotron one without detailed numerical simulations.⁶ After the plateau phase, u_{soft} drops dramatically and we expect the synchrotron losses to be dominant.

⁶ Should the IC losses dominate, E_e^{max} and $E_{v,\text{syn}}^{\text{max}}$ are to be reduced by the factors $\xi^{1/2}$ and ξ , respectively.

For photons with energy $E_\nu \leq m_e c^2 \sim 0.5$ MeV, the main source of opacity is the Compton scattering in the Thomson regime. The corresponding optical depth is

$$\tau_T \simeq \sigma_T M_{\text{ej}} / 4\pi m_p (t v_{\text{ej}})^2 \simeq 6 M_{\text{ej},1} t_7^{-2} v_{\text{ej},9}^{-2}, \quad (75)$$

where σ_T is the Thomson cross-section. Thus, the shell becomes transparent in about 1 yr after the explosion. The typical energy of photons from radioactive decays is around 1 MeV and hence the ejecta opacity to these photons is similar. As a result, the synchrotron photons and the photons from radioactive decays are utilized with similar efficiency.

When $E_\nu \gg m_e c^2$ the scattering is in the Klein–Nishina regime and the cross-section is smaller, $\sigma_{\text{KN}} \approx 3\sigma_T m_e c^2 / 8E_\nu$ (Lang 1980). For 100-MeV synchrotron photons, this yields

$$\tau_{\text{KN}} \simeq 10^{-2} M_{\text{ej},1} t_7^{-2} v_{\text{ej},9}^{-2} \quad (76)$$

and these photons begin to escape already after 10 d or so. However, provided the spectrum of the shock-accelerated electrons is a power law $N(E) \propto E^{-p}$ with $p > 2$, which is expected to be the case, the contribution of such highly energetic photons to the energy transport is lower.

The IC photons with energy $E_\nu > (2m_e c^2)^2 / E_{\nu,\text{soft}} \simeq 1.2$ TeV will also interact with the soft supernova photons via the two-photon pair-production reaction (here we used $E_{\nu,\text{soft}} = 1$ eV). The corresponding opacity can be estimated as

$$\tau_{\gamma\gamma} \simeq \frac{\sigma_T}{5} \frac{L_{\text{soft}}}{4\pi (v_{\text{ej}} t) c E_{\text{soft}}} \simeq 2 L_{\text{soft},41} v_{\text{ej},9}^{-1} t_7^{-1}. \quad (77)$$

Thus, we expect the ejecta to become transparent to the IC emission soon after the end of the plateau phase.

The above calculations show that during the plateau phase the high-energy emission from the termination shock of the magnetar wind is deposited in the ejected envelope. However, this additional heating has little effect on the supernova luminosity. Indeed, the increase in the luminosity due to this heating can be estimated as

$$\Delta L \simeq \frac{E_{\text{rot}}(t)t}{t_d^2} \simeq \frac{L_w(t)t^2}{t_d^2} = L_w(t_d) \ll L. \quad (78)$$

For $t > t_d$ the energy deposition rate does no longer scale as t^{-2} (cf. Woosley 2010) as the ejecta becomes transparent to the high-energy emission. For example, if the synchrotron emission is the main channel of heating, then the rate scales as $L_w \tau \propto t^{-4}$ when $\tau < 1$, and the rate due to IC emission is likely to decline even faster.

Out of the well-studied supernovae known to the authors, none fits the above description. The closest example is SN 1994W (Cortini et al. 1994; Sollerman et al. 1998). This is one of the brightest Type II supernovae with the peak luminosity $\sim 10^{43}$ erg s $^{-1}$. After around 120 d its luminosity drops dramatically down to $\sim 10^{41}$ erg s $^{-1}$. The tail of its light curve is very steep showing very small mass of the ejected ^{56}Ni (Sollerman et al. 1998). In fact the data can be approximated by $L \propto t^{-4.6}$. All these properties agree nicely with our expectations. On the negative side, the spectral data indicate the lower ejecta speed and the presence of a very slow component with $v \sim 1000$ km s $^{-1}$. This supernova is classified as Type II_n and seems to be explained very well in the model involving a collision between the SN ejecta and a massive circumstellar shell ejected few years earlier in the giant stellar eruption (Chugai et al. 2004; Smith et al. 2007, 2008; Woosley et al. 2007).

The power of the escaped high-energy emission can be estimated as $L_\nu \simeq L_w e^{-\tau}$. As usual in such cases, it will peak when $\tau \sim 1$, which may occur within the first year after the explosion. For a source at the distance $d = 10d_1$ Mpc, the corresponding total flux

will be

$$F^{\text{peak}} \simeq 3 \times 10^{-12} B_{\text{NS},15}^{-2} t_{\text{p},7}^{-2} d_1^{-2} \text{ erg cm}^{-2} \text{ s}^{-1}, \quad (79)$$

where t_p is the time when the peak is reached. For the synchrotron component, the spectral energy distribution is expected to peak around $E_\nu = 100$ keV (see equation 70).

4.4 Remnant

What is left behind after the explosion depends on where inside the RSG it occurs. As we have demonstrated, this strongly depends on the mean specific angular momentum of the gas captured via the Bondi–Hoyle mechanism. If it is as high as proposed in the early investigations (Illarionov & Sunyaev 1975; Shapiro & Lightman 1976), then the NS will accrete only at the Eddington rate until it settles into the core of its companion. What would happen after this is not clear. The current view is that the neutrino cooling will be sufficiently high for the accretion to proceed at the Bondi rate and that the NS collapses into a BH (Zel’dovich, Ivanova & Nadezhin 1972). However, this conclusion is based on spherically symmetric models. The high rotation rate developed in the core of the primary during the in-spiral means that instead of directly accreting on to the NS the core will form a torus, whose neutrino cooling may not be very effective, in which case such a configuration can be relatively long-lived. Moreover, the mass accretion will be accompanied by the efficient recycling of the NS, so one can still expect the NS to turn into a millisecond magnetar before its mass becomes high enough for gravitational collapse. Even if the magnetar-driven explosion fails in the dense environment of the core, and the NS eventually collapses into a BH, this will be a rapidly rotating BH accompanied by a massive accretion disc – the configuration characteristic of the collapsar model for a GRB. However, in contrast to the GRB progenitors, the envelope of the RSG star is not sufficiently compact for the relativistic jet to penetrate it during the typical lifetime of the GRB central engine. Instead, the jet energy will be deposited in the RSG envelope and most likely result in a supernova explosion, leaving behind a BH remnant. Interestingly, the mass of the pre-supernova could be below the limit for BH formation in the normal course of its evolution as a solitary star.

If the angular momentum is much lower, as suggested by Davies & Pringle (1980), then the explosion occurs when the NS is still inside the RSG envelope and then the remnant is likely to be a close binary consisting of a WR star and a magnetar.⁷ In order to show this, we first note that the pressure inside the core of the RSG at the He-burning phase is $p_c \sim 10^{19}$ erg cm $^{-3}$ and much higher at the pre-supernova phase (Woosley et al. 2002). This has to be compared with the pressure inside the high-entropy bubble, created by the magnetar,

$$p_b \simeq \frac{L_w t}{4\pi R_b^3} \quad (80)$$

where $R_b = v_b t$ is the bubble radius, v_b is its expansion speed and t is the time since the explosion. We are interested in its value at the time when the bubble radius is comparable with the separation between the NS and the RSG core. Taking $R_p = 10^{10} R_{b,10}$ cm and $t = R_b / v_b$, we find that

$$p_b \simeq 10^{19} L_{w,49} v_{b,9}^{-1} R_{b,10}^{-2} \text{ erg cm}^{-3}. \quad (81)$$

⁷ The 2D numerical simulations by Fryer et al. (1996) have indicated the possibility of a neutrino-driven explosion during the CE phase, also leaving behind a close binary system.

If the explosion occurs while the NS is still well inside the RSG envelope, then $R_{b,10} \gg 1$ and $P_b < P_c$. Thus, the magnetar wind cannot destroy the core. Another point is whether the gravitational coupling between the NS and the core is strong enough for the binary to survive the high mass-loss during the explosion. Such a destruction is unlikely because for a sufficiently small separation at the time of the explosion most of the mass-loss will come from the envelope, which has no effect on the gravitational attraction between the NS and the core.

The magnetar wind will interact with the WR wind and will terminate when the radius of magnetar magnetosphere drops below the light cylinder radius. The magnetospheric radius is determined by the pressure balance

$$\frac{B_{\text{NS}}^2}{8\pi} \left(\frac{R_m}{R_{\text{NS}}} \right)^{-6} = \frac{\dot{M}_{\text{WR}} v_{\text{WR}}}{4\pi a^2}, \quad (82)$$

which yields

$$R_m \simeq 6 \times 10^9 B_{\text{NS},15}^{1/3} \dot{M}_{\text{WR},-5}^{-1/6} v_{\text{WR},8}^{-1/6} a_{11}^{1/3} \text{ cm}. \quad (83)$$

Using equation (66) to find the light cylinder radius, we estimate the termination time of the magnetar wind as

$$t_w \simeq 25 B_{\text{NS},15}^{-4/3} \dot{M}_{\text{WR},-5}^{-1/3} v_{\text{WR},8}^{-1/3} a_{11}^{2/3} \text{ yr}. \quad (84)$$

The Bondi–Hoyle accretion radius of the magnetar in the WR wind

$$R_A = \frac{2GM}{v_{\text{WR}}^2} \simeq 4 \times 10^{10} v_{\text{WR},8}^{-2} \text{ cm} \quad (85)$$

is above the magnetospheric radius, indicating that the magnetar may begin to accrete when its corotation radius

$$R_{\text{cor}} = \left(\frac{GM}{\Omega^2} \right)^{1/3} \simeq 5 \times 10^9 B_{\text{NS},15}^{2/3} t_{13}^{1/3} \text{ cm} \quad (86)$$

exceeds R_m . Ignoring the decay of the magnetar’s magnetic field, we find that this will occur at

$$t \simeq 7 \times 10^5 B_{\text{NS},15}^{-1} \dot{M}_{\text{WR},-5}^{-1/2} v_{\text{WR},8}^{-1/2} a_{11} \text{ yr}. \quad (87)$$

In fact, this time exceeds the expected decay time of the magnetar magnetic field

$$t_{\text{dec}} \simeq 10^4 B_{15}^{-2} \text{ yr} \quad (88)$$

(Heyl & Kulkarni 1998). However, the relatively weak dependence of R_m on B_{NS} indicates that the effect of magnetic field decay is minor and for the whole duration of the WR phase of the companion the magnetar will not be accreting. Instead, the magnetar will exhibit the behaviour typical for soft gamma-ray repeaters or anomalous X-ray pulsars (Thompson & Duncan 1996).

Normally, a close high-mass binary system can produce at most two supernovae. However, our results suggest that in some cases this number can be increased to three. Indeed, in our model, the first explosion creates the NS itself. When this NS spirals into its companion, the second, now off-centre, explosion occurs. Finally, when the core of the WR star eventually collapses, there is another explosion. Moreover, the very close separation between the magnetar and WR star makes this binary system a promising GRB progenitor (e.g. Barkov & Komissarov 2010). Indeed, the WR star is very compact so the relativistic GRB jets can break out in a reasonably short time and the spin–orbital interaction ensures that the WR star is rapidly rotating. These are the two most important properties which a long GRB progenitor must have.

5 CONCLUSIONS

The main aim of this study was to investigate whether during the CE phase of a close binary, involving a RSG and NS, the NS can spin up to a millisecond period and generate magnetar-strength magnetic field. If possible, this would result in magnetically driven stellar explosion, releasing up to 10^{52} erg of the magnetar’s rotational energy inside the RSG.

It turns out that the outcome is very sensitive to the specific angular momentum of the gas gravitationally captured by the NS during the in-spiral. Should it be as high as suggested in the early papers by Illarionov & Sunyaev (1975) and Shapiro & Lightman (1976), the accretion rate is low and neither the mass nor the spin of the NS will increase significantly until the NS settles into the centre of the RSG. This is because the accretion disc forms too far from the NS, its temperature remains rather low, and it is unable to cool effectively via neutrino emission, which is very sensitive to temperature. As a result, the accretion shock is pushed too far, beyond the sonic point of the Bondi-type flow, thus preventing the accretion from reaching the Bondi–Hoyle rate (Chevalier 1996). The CE can either be ejected, leaving behind a close NS–WR binary, or survive, leading to a merger of the NS with the RSG core (Taam & Sandquist 2000). It is not clear what exactly would occur following the merger, as we cannot treat this case using our approach. The common belief is that the NS will begin to accrete at the Bondi rate and collapse into a BH. However, this conclusion is based on models with spherical symmetry, whereas the strong rotation developed by the system during the merger makes the assumption of spherical symmetry unsuitable. It may still be possible that the NS spins up to a millisecond period and becomes a magnetar before its mass reaches the limit of gravitational collapse.

If, on the contrary, the angular momentum is much lower, more in line with the analysis of Davies & Pringle (1980), the accretion can begin to proceed at the Bondi–Hoyle rate when the NS is still inside the CE. Further investigations of the Bondi–Hoyle accretion via 3D numerical simulations are required to clarify this issue.

Once the NS becomes a millisecond magnetar, its emerging magnetosphere interacts with the accretion flow. If this occurs while the NS is still inside the CE and the magnetic field is as strong as $\sim 10^{15}$ G, the interaction is most likely to begin in the propeller regime and then quickly proceed to the ejector regime, given the small radius of the light cylinder. Strong magnetar wind blows away the CE and drives an explosion whose energy is likely to exceed the standard 10^{51} erg of normal supernovae. However, the core of the companion survives and the explosion leaves behind a very close binary, consisting of a magnetar and a WR star. In spite of the very close separation and the very strong wind from the WR star, the NS is shielded from the wind by its magnetosphere and prevented from accreting. Later on, when the WR star explodes, this will be a *third* explosion produced in the system. Moreover, the rapid rotation and the compactness of this WR star show that this explosion can be accompanied by a GRB (Barkov & Komissarov 2010).

If the magnetar forms only after the merger with the core, then a higher magnetic field, $\sim 10^{16}$ G, is required to explode the star. In this case, the remnant is a solitary magnetar. If, however, the magnetar-driven explosion fails and the NS collapses into a BH, this will be a rapidly rotating BH with a massive accretion disc. Although this is exactly the configuration proposed in the collapsar model of GRBs, the relativistic jets will not be able to escape from the extended envelope of the RSG and produce such a burst. Instead, they will deposit their energy inside the envelope and drive a Type II supernova.

Given the very high rotational energy of a millisecond NS, the supernova is expected to be very bright at the plateau phase and show very broad spectral lines. However, only a small amount of ^{56}Ni is expected to be produced in the explosion due to the relatively low densities, in comparison to those reached during the normal core-collapse explosions. By the end of the plateau phase, the power of the magnetar wind is also significantly reduced and the supernova brightness is expected to drop sharply. The combination of the rapidly declining power of the magnetar wind and the increasing transparency of the supernova ejecta to the high-energy emission from the wind termination shock results in steeper-than-normal light-curve tails.

The unique property of supernovae produced in this way is the high-energy synchrotron and IC emission from the MWN. Unfortunately, the supernova ejecta does not become transparent to this emission until a hundred days after the explosion, by which time the NS rotation is already very slow and its wind is no longer that powerful. The flux of the gamma-ray emission is expected to be rather low and difficult to observe, unless the explosion occurs in the Local Group of galaxies.

ACKNOWLEDGMENTS

We are thankful to V. Bosch-Ramon, N. Ikhshanov and Y. Levin for fruitful discussions, as well as to A. Heger for providing models of RSGs. The calculations were fulfilled at the cluster of the Moscow State University ‘Chebyshev’. This research was funded by the STFC under the Rolling Programme of Astrophysical Research at Leeds University.

REFERENCES

- Akiyama S., Wheeler J. C., Meier D. L., Lichtenstadt I., 2003, *ApJ*, 584, 954
- Alpar M. A., Cheng A. F., Ruderman M. A., Shaham J., 1982, *Nat*, 300, 728
- Archibald A. M. et al., 2009, *Sci*, 324, 1411
- Arras P., Flanagan E. E., Morsink S. M., Schenk A. K., Teukolsky S. A., Wasserman I., 2003, *ApJ*, 591, 1129
- Backer D. C., Kulkarni S. R., Heiles C., Davis M. M., Goss W. M., 1982, *Nat*, 300, 615
- Bahcall J. N., 1964, *Phys. Rev.*, 136, 1164
- Balbus S. A., Hawley J. F., 1991, *ApJ*, 376, 214
- Barkov M. V., 2008, in Axelsson M., ed., *AIP Conf. Ser. Vol. 1054, Cool Discs, Hot Flows: The Varying Faces of Accreting Compact Objects*. Am. Inst. Phys., New York, p. 79
- Barkov M. V., Komissarov S. S., 2010, *MNRAS*, 401, 1644
- Barkov M. V., Bisnovatyi-Kogan G. S., Lamzin S. A., 2001, *Astron. Rep.*, 45, 230
- Bisnovatyi-Kogan G. S., Komberg B. V., 1974, *SvA*, 18, 217
- Bisnovatyi-Kogan G. S., Syunyaev R. A., 1971, *AZh*, 48, 881
- Bondarescu R., Teukolsky S. A., Wasserman I., 2007, *Phys. Rev. D*, 76, 064019
- Brink J., Teukolsky S. A., Wasserman I., 2005, *Phys. Rev. D*, 71, 064029
- Brown E. F., 2000, *ApJ*, 531, 988
- Brown G. E., Weingartner J. C., 1994, *ApJ*, 436, 843
- Bucciantini N., Thompson T. A., Arons J., Quataert E., Del Zanna L., 2006, *MNRAS*, 368, 1717
- Burrows A., Dessart L., Livne E., Ott C. D., Murphy J., 2007, *ApJ*, 664, 416
- Chakrabarty D., Morgan E. H., Muno M. P., Galloway D. K., Wijnands R., van der Klis M., Markwardt C. B., 2003, *Nat*, 424, 42
- Chandrasekhar S., 1961, *Hydrodynamic and Hydromagnetic Stability*. Clarendon, Oxford
- Chevalier R. A., 1993, *ApJ*, 411, L33
- Chevalier R. A., 1996, *ApJ*, 459, 322
- Chugai N. N. et al., 2004, *MNRAS*, 352, 1213

- Cortini G., Villi M., Barbon R., Munari U., Bragaglia A., Pollas C., 1994, *IAU Circ.*, 6042, 1
- Davies R. E., Pringle J. E., 1980, *MNRAS*, 191, 599
- de Jager O. C., Harding A. K., Michelson P. F., Nel H. I., Nolan P. L., Sreekumar P., Thompson D. J., 1996, *ApJ*, 457, 253
- Demorest P. B., Pennucci T., Ransom S. M., Roberts M. S. E., Hessels J. W. T., 2010, *Nat*, 467, 1081
- Dicus D. A., 1972, *Phys. Rev. D*, 6, 941
- Duncan R. C., Thompson C., 1992, *ApJ*, 392, L9
- Fryer C. L., Woosley S. E., 1998, *ApJ*, 501, 780
- Fryer C. L., Benz W., Herant M., 1996, *ApJ*, 460, 801
- Gnedin O. Y., Yakovlev D. G., Potekhin A. Y., 2001, *MNRAS*, 324, 725
- Heger A., Woosley S. E., Langer N., Spruit H. C., 2004, in Maeder A., Eenens P., eds, *Proc. IAU Symp. 215, Stellar Rotation*. Astron. Soc. Pac., San Francisco, p. 591
- Heyl J. S., Kulkarni S. R., 1998, *ApJ*, 506, L61
- Houck J. C., Chevalier R. A., 1991, *ApJ*, 376, 234
- Hoyle F., Lyttleton R. A., 1939, *Proc. Camb. Phil. Soc.*, 34, 405
- Illarionov A. F., Sunyaev R. A., 1975, *A&A*, 39, 185
- Inogamov N. A., Sunyaev R. A., 1999, *Astron. Lett.*, 25, 269
- Inogamov N. A., Sunyaev R. A., 2010, *Astron. Lett.*, 36, 848
- Ishii T., Matsuda T., Shima E., Livio M., Anzer U., Boerner G., 1993, *ApJ*, 404, 706
- Jacoby B. A., Hotan A., Bailes M., Ord S., Kulkarni S. R., 2005, *ApJ*, 629, L113
- Kasen D., Bildsten L., 2010, *ApJ*, 717, 245
- Kaspi V. M., Taylor J. H., Ryba M. F., 1994, *ApJ*, 428, 713
- Kennel C. F., Coroniti F. V., 1984, *ApJ*, 283, 694
- Komissarov S. S., Barkov M. V., 2007, *MNRAS*, 382, 1029
- Komissarov S. S., Lyutikov M., 2011, *MNRAS*, doi:10.1111/j.1365-2966.2011.18516.x
- Kouveliotou C. et al., 1998, *Nat*, 393, 235
- Lang K. R., 1980, *Astrophysical Formulae. A Compendium for the Physicist and Astrophysicist*. Springer-Verlag, Berlin
- Lattimer J. M., Prakash M., 2007, *Phys. Rep.*, 442, 109
- Levin Y., 1999, *ApJ*, 517, 328
- MacFadyen A. I., Woosley S. E., 1999, *ApJ*, 524, 262
- Magkotsios G., Timmes F. X., Hungerford A. L., Fryer C. L., Young P. A., Wiescher M., 2010, *ApJS*, 191, 66
- Metzger B. D., Thompson T. A., Quataert E., 2007, *ApJ*, 659, 561
- Mineshige S., Rees M. J., Fabian A. C., 1991, *MNRAS*, 251, 555
- Obergaulinger M., Cerdá-Durán P., Müller E., Aloy M. A., 2009, *A&A*, 498, 241
- Paczynski B., 1976, in Eggleton P., Mitton S., Whelan J., eds, *Proc. IAU Symp. 73, Structure and Evolution of Close Binary Systems*. Reidel, Dordrecht, p. 75
- Postnov K. A., Yungelson L. R., 2006, *Living Rev. Relativ.*, 9, 6
- Rezzolla L., Giacomazzo B., Baiotti L., Granot J., Kouveliotou C., Aloy M. A., 2011, *ApJ*, 732, L6
- Ruffert M., 1997, *A&A*, 317, 793
- Ruffert M., 1999, *A&A*, 346, 861
- Shapiro S. L., 2000, *ApJ*, 544, 397
- Shapiro S. L., Lightman A. P., 1976, *ApJ*, 204, 555
- Shapiro S. L., Teukolsky S. A., 1983, *Black Holes, White Dwarfs, and Neutron Stars: The Physics of Compact Objects*. Wiley, New York
- Shima E., Matsuda T., Takeda H., Sawada K., 1985, *MNRAS*, 217, 367
- Smith N. et al., 2007, *ApJ*, 666, 1116
- Smith N., Chornock R., Li W., Ganeshalingam M., Silverman J. M., Foley R. J., Filippenko A. V., Barth A. J., 2008, *ApJ*, 686, 467
- Sollerman J., Cumming R. J., Lundqvist P., 1998, *ApJ*, 493, 933
- Spitkovsky A., 2006, *ApJ*, 648, L51
- Spruit H. C., 1999, *A&A*, 341, L1
- Taam R. E., Sandquist E. L., 2000, *ARA&A*, 38, 113
- Thompson C., Duncan R. C., 1993, *ApJ*, 408, 194
- Thompson C., Duncan R. C., 1996, *ApJ*, 473, 322
- Thompson T. A., Burrows A., Meyer B. S., 2001, *ApJ*, 562, 887
- Thompson T. A., Chang P., Quataert E., 2004, *ApJ*, 611, 380
- Thorne K. S., Zytkov A. N., 1977, *ApJ*, 212, 832

Thorsett S. E., Chakrabarty D., 1999, *ApJ*, 512, 288
Tsvetkov D. Y., 1995, *Inf. Bull. Var. Stars*, 4253, 1
Tutukov A. V., Yungelson L. R., 1979, *Acta Astron.*, 29, 665
Usov V. V., 1992, *Nat*, 357, 472
Ustyugova G. V., Koldoba A. V., Romanova M. M., Lovelace R. V. E., 2006, *ApJ*, 646, 304
Woosley S. E., 2010, *ApJ*, 719, L204

Woosley S. E., Heger A., Weaver T. A., 2002, *Rev. Mod. Phys.*, 74, 1015
Woosley S. E., Blinnikov S., Heger A., 2007, *Nat*, 450, 390
Zel'dovich Y. B., Ivanova L. N., Nadezhin D. K., 1972, *SvA*, 16, 209
Zhang W., Fryer C. L., 2001, *ApJ*, 550, 357

This paper has been typeset from a $\text{\TeX}/\text{\LaTeX}$ file prepared by the author.